HHS Public Access

Author manuscript

J Acquir Immune Defic Syndr. Author manuscript; available in PMC 2022 December 01.

Published in final edited form as:

J Acquir Immune Defic Syndr. 2021 December 01; 88(4): 414–419. doi:10.1097/QAI.0000000000002783.

Modeling the Effects of HIV and Aging on Resting-State Networks using Machine Learning

Patrick H. Luckett, PhD[1], **Robert H. Paul, PhD**[2], **Kayla Hannon, BS**[1], **John J. Lee, MD**[3], **Joshua S. Shimony, MD**[3], **Karin L. Meeker, PhD**[1], **Sarah A. Cooley, PhD**[1], **Anna H. Boerwinkle, BS**[1], **Beau M. Ances, MD, PhD**[1]

[1]Department of Neurology, Washington University School of Medicine, St. Louis, Missouri

[2]Department of Psychological Sciences, University of Missouri Saint Louis, St. Louis, Missouri

[3]Mallinckrodt Institute of Radiology, Washington University School of Medicine, St. Louis, Missouri

Abstract

Background: The relationship between HIV infection, the functional organization of the brain, cognitive impairment, and aging remains poorly understood. Understanding disease progression over the lifespan is vital for the care of people living with HIV (PLWH).

Setting: Virologically suppressed PLWH (n=297) on combination antiretroviral therapy and 1509 HIV uninfected healthy controls were evaluated. PLWH were further classified as cognitively normal (CN) or impaired (CI) based on neuropsychological testing.

Methods: Feature selection identified resting state networks (RSNs) that predicted HIV and cognitive status within specific age bins (< 35, 35–55, >55). Deep learning models generated voxelwise maps of RSNs to identify regional differences.

Results: Salience (SAL) and parietal memory networks (PMN) differentiated individuals by HIV status. When comparing controls to PLWH CN the PMN and SAL had the strongest predictive strength across all ages. When comparing controls to PLWH CI SAL, PMN, and frontal parietal (FPN) were the best predictors. When comparing PLWH CN to PLWH CI SAL, FPN, basal ganglia, and ventral attention were the strongest predictors. Only minor variability in predictive strength was observed with aging. Anatomically, differences in RSN topology occurred primarily in the dorsal and rostral lateral prefrontal cortex, cingulate, and caudate.

Conclusion: Machine learning identified RSNs that classified individuals by HIV and cognitive status. PMN and SAL were sensitive for discriminating HIV status, with involvement of FPN occurring with cognitive impairment. Minor differences in RSN predictive strength were observed by age. These results suggest specific RSNs are affected by HIV, aging, and HIV associated cognitive impairment.

Keywords

Machine learning; HIV; resting state functional connectivity; cognitive impairment; aging

Corresponding Author: Patrick H. Luckett, PhD, Department of Neurology, Campus Box 8111, 660 S. Euclid Avenue, St. Louis, MO 63110, Phone: 314-747-8423, Fax: 314-747-8427, luckett.patrick@wustl.edu.

Introduction

More than 37 million people worldwide have HIV[1]. HIV affects the brain soon after seroconversion and leads to chronic neuro-inflammation[2]. Treatment with combination antiretroviral therapy (cART) can slow the progression of the disease and reduces the risk of transmission. Due to effective treatment with cART, the average life expectancy of people living with HIV (PLWH) is now similar to HIV uninfected (HIV-) individuals. This has turned HIV from a fatal disease for most individuals into a more chronic condition[3].

Despite the success of cART, milder forms of cognitive impairment persist that involve multiple domains[4]. The presence of cognitive impairment may result from multiple mechanisms including psychosocial factors, mechanisms that predated HIV and/or cART (legacy effects), continued low level inflammation despite cART, and/or the presence of viral reservoirs[4]. Consequently, identifying changes in brain structure and function across the lifespan of PLWH remains important.

Studies have shown that spontaneous correlated patterns of neural oscillations are a consistent feature of brain networks associated with numerous brain functions. These include information transfer, mechanisms of plasticity, and support of cognitive functions[5]. Resting-state functional connectivity (RS-FC), which measures the temporal relationship of blood oxygen level dependent (BOLD) fluctuations, is reflective of the neural organization of the brain and can be parcellated into resting state networks (RSNs)[6]. RS-FC allows for the evaluation of a hierarchy of topological boundaries that define the functional organization of the brain.

Alterations in the temporal and spatial patterns of RS-FC vary across the lifespan and by medical condition[7]. In HIV, abnormal RS-FC has been observed within cortical and subcortical brain regions that comprise multiple RSNs, including the default mode, sensory, motor, and attention networks. Alterations in RSNs associate with cognitive impairment due to HIV, possibly reflecting loss of some connections and compensatory recruitment of networks to support cognitive function[6,8].

The use of data driven machine learning (ML) models has become common in the medical field. These methods avoid heuristics, are noise tolerant, and are robust to feature interactions[9]. While most statistical analyses have primarily focused on group-level differences, ML algorithms can be tailored to identify contrasts at the individual level which has potential to support personalized clinical care[10]. To design such personalized treatments, we need to first understand the critical determinants. Feature selection is designed to identify and characterize relationships that are most relevant to a particular outcome. Multiple studies have used ML to reveal novel mechanisms and associations relevant to HIV[11,12].

This study utilizes ML based feature selection within a large cohort of PLWH on cART who were virologically controlled (<200 copies/mL) (n=297) and 1509 controls to identify RSNs that distinguish between HIV serostatus (controls compared to cognitively normal PLWH (PLWH CN), and controls compared to cognitively impaired PLWH (PLWH CI) with respect to different age bins (< 35 years old, 35–55 years old, and >55 year old). Further, we identified the RSNs that are the strongest predictors of cognitive status between PLWH CN

and PLWH CI across different ages. Lastly, a deep learning model generated voxelwise maps of RSNs that identified salient changes in RSN topology amongst the three groups. This data-driven approach presents an opportunity to uncover novel disease trajectories relevant to HIV infection.

Methods

Participants

PLWH were selected from ongoing studies conducted by the Infectious Disease Clinic at Washington University in Saint Louis (WUSTL). A participant was excluded if (s)he were younger than 18 years old, had a history of confounding neurological disorders, had current or past opportunistic central nervous system (CNS) infections, had traumatic brain injury with loss of consciousness >30 minutes, had major psychiatric disorders, or met criteria for current substance use disorder according to the Diagnostic and Statistics Manual of Mental Disorders 5th edition. All PLWH were on stable cART for at least 6 months and had a recent viral load <200 copies/mL. Studies involving PLWH collected neuroimaging data at the same institution on the same type of scanner with the same scanning protocols. All of these studies followed similar neuropsychological and blood/CSF lab protocols. RS-FC was acquired from control participants (N=1806) through ongoing research studies conducted at WUSTL, as well as the Brain Genomics Superstruct Project[13]. The appropriate Institutional Review Boards approved all studies, and all participants provided written informed consent.

Neuropsychological assessment

For all PLWH, neuropsychological testing targeted five neurocognitive domains previously described[11]. A total of 15 tests were administered, including: 1) *learning*: total recall across the learning trials on the Hopkins Verbal Learning Test-Revised (HVLT-R) and Brief Visuospatial Memory Test-Revised (BVMT-R); 2) *memory*: delayed recall on the HVLT-R and BVMT-R; 3) executive: Trail Making Test B, Letter-Number Sequencing, Verb Fluency, and Color Word Interference Test Trial 3; 4) *motor/psychomotor speed*: Trail Making Test A, Digit Symbol, grooved pegboard dominant and non-dominant hands, and Symbol Search; 5) *language*: letter fluency (FAS) and category fluency (animals). Time to completion or total correct served as the dependent measures in accord with standard methods. Raw test scores were transformed into Z-scores using published norms corrected for age, education, sex, and race. PLWH who had at least one domain Z-score < −2 or two domain Z-scores < −1 were designated as cognitively impaired.

Normative cognitive status for the control participants was confirmed by a structured clinical rating scale (i.e., the Clinical Dementia Rating Scale (CDR® [14]) or online cognitive test protocol[13]. These tests results were only used to confirm normal cognition for the control participants.

Magnetic resonance imaging (MRI) acquisition

All neuroimaging was performed on a 3T Siemens MR Scanner (Siemens AG, Erlangen, Germany) equipped with a standard 12-channel head coil. A high-resolution, three-dimensional, sagittal, T1-weighted, magnetization-prepared rapid gradient echo (MPRAGE)

scan was acquired (echo time [TE] = 16 ms, repetition time [TR] = 2,400 ms, inversion time = 1,000 ms, flip angle = 8°, 256 × 256 acquisition matrix, 1 mm^3 voxels). RS-FC scans were collected using an echo planar sequence (voxel size = 3–4 mm^3, TR = 2200–3000 ms, FA = 80°−90°) that is sensitive to BOLD contrast. Each participant had approximately 14 min of RS-FC data.

MRI processing

Structural data preprocessing was completed using FreeSurfer version 5.3 (http://surfer.nmr.mgh.harvard.edu) as previously described[11]. Visual inspection of automated segmentation results was performed for quality assurance and corrections were made when necessary. RS-FC preprocessing methods were performed as previously described[15,16]. Head motion was corrected utilizing affine transformations, and additional in-house methods were used to exclude participants with excessive head movement. Data also underwent nuisance regressors using whole brain signal, ventricular (CSF) and white matter signal, movement time-series, and low-pass temporal filtering to remove frequencies above 0.08 Hz. The structural MPRAGE and preprocessed RS-FC scans were cross-aligned using boundary-based registration. A 4-mm full-width half-maximum smoothing kernel was used in the surface space.

Predefined regions of interest (ROIs)[17] were used to assess RS-FC in cortical and subcortical regions. A total of 300 ROIs encompassing 15 RSNs (dorsal somatomotor (SMD), ventral somatomotor (SMV), cinguloopercular (CON), auditory (AUD), default mode (DMN), parietal memory (PMN), visual (VIS), frontoparietal (FPN), salience (SAL), ventral attention (VAN), dorsal attention (DAN), medial temporal (MET), reward (REW), basal ganglia (BGN), and thalamus (THA)) were included. A similarity map was obtained by computing the Pearson's correlation between BOLD time series from the 300 ROIs. Averaging between-network and within-network correlations produced a similarity map for the 15 RSNs.

Feature selection

RSNs were ranked according to their predictive value using a Relief algorithm[18]. Additional details can be found in supplementary material. Features were evaluated according to different age groups (<35 years old, 35–55 years old, >55 years old). Input to the Relief algorithm included the 120 RS-FC correlations from the 15 RSNs for participants within a given age group. Comparing PLWH with controls, the response variable was HIV status. When comparing between the two PLWH groups, the response variable was cognitive impairment status. To rank the importance of RSNs, all within and between network weights for the 15 RSNs were averaged to generate an aggregate input feature. The aggregate features with an average weight ≥ 0.5 were considered strong predictors. Feature weights were validated on 5 iterations with different subsets of data.

Deep learning

A three-dimensional convolutional neural network (3DCNN) was trained to generate voxelwise maps of RSNs. Training and validation of the model are described in supplementary material. In short, random subsampling of ROIs within a given predefined

network was used to extract a 3D similarity map by computing the Pearson's correlation between the mean of the subsampled BOLD signals and every other voxel in the brain. The 3D similarity map was then assigned to one of the 15 RSNs based on the highest correlation between the subsampled signal and the signal for each RSN. The resulting RSN maps represent the probability of a given voxel belonging to each of the 15 RSNs. The 3DCNN was implemented in Matlab R2019b (www.mathworks.com). Supplemental figure 1 summarizes the analysis process outlined in this research.

Results

Demographics of the cohort

The majority of the control cohort (N=1509) were males (62%) with an average age of 45.4 (±23.6) years. The majority of the PLWH CN cohort (N=181) were males (65%) with an average age of 50.5 (±12.9) years. The majority of the PLWH CI cohort (N=116) were males (69%) with an average age of 44.6 (±14.4) years. Detailed demographics are presented in Table 1.

Controls compared to PLWH CN

Figure 1 (red bars) shows the results of the Relief algorithm when comparing controls to PLWH CN. The bar heights represent the relative importance of each RSN in differentiating individuals as either controls or PLWH with normative cognitive performance, with a "1" indicating the strongest predictive network. The PMN, SAL, and VIS were the RSNs that had the strongest predictive ability for differentiating the two groups. A voxel-wise analysis of topographic changes in the SAL revealed that the group difference was driven mostly by alterations in connectivity in the anterior cingulate cortex (ACC) and the dorsolateral prefrontal cortex (DLPFC) (Figure 2). For the PMN the greatest differences were observed in parietal regions and the retrosplenial cortex (Figure 3). Lastly, for VIS the greatest difference was in the occipital lobe. The PMN and VIS were important discriminators across all bins. The SAL was a moderately strong predictor in the younger age group (<35), and became a stronger predictor with age (>35).

Controls compared to PLWH CI

Figure 1 (yellow bars) shows the results of the Relief algorithm when comparing controls to PLWH CI. The PMN, SAL, and FPN differentiated these two groups. Voxel-wise analysis of topographic changes identified the largest anatomical differences in the SAL, which included both the ACC and DLPFC (Figure 2). Voxelwise maps of the PMN showed that the largest differences were in parietal regions and the retrospenial cortex (Figure 2). Differences in the FPN were primarily in the DLPFC, rostral lateral prefrontal cortex (RLPFC), and portions of the parietal lobule (Figure 3). The PMN and SAL maintained their strong predictive strength across the age bins. While the FPN was a strong predictor in all age groups, it had reduced predictive strength for older ages.

PLWH CN compared to PLWH CI

Figure 1 (green bars) shows the results comparing PLWH CN to PLWH CI with cognitive impairment being the main discriminator. The REW, SAL, VAN, FPN, BGN, and VIS

differentiated PLWH according to cognitive impairment status. Voxel-wise analysis of topographic changes in the SAL identified the greatest differences occurred in the ACC and the DLPFC (Figure 2). Differences in the FPN were primarily in the RLPFC and portions of the parietal lobule (Figure 3). Differences observed in the BGN were primarily seen in the caudate, globus pallidus, and posterior putamen. Differences in the REW were seen in the ventromedial prefrontal cortex, amygdala, nucleus accumbens, and orbitofrontal regions. Each of these networks were important determinants of cognitive status across age bins.

Discussion

This study identified several novel findings with regards to changes in the functional organization of the brain in the context of HIV status, cognitive impairment, and age. The strongest RSNs that were predictive for each of the comparisons included: the SAL, PMN, and VIS when comparing controls and PLWH CN; SAL, PMN, and FPN when comparing controls and PLWH CI; and the REW, SAL, VAN, FPN, BGN, and VIS when comparing PLWH CN to PLWH CI. Multiple RSNs were associated with cognitive impairment when comparing PLWH CN to PLWH CI. The RSNs that had the strongest predictive ability across the age spectrum or became stronger with increasing age were the SAL, PMN, and FPN. However, anatomical variability occurred in network strength with respect to the different age groups (Figure 2–4). These results point to a complex phenotype imposed by HIV infection, even with viral suppression with cART.

When comparing controls to PLWH CN with HIV status, the PMN, SAL, and VIS networks were the strongest differentiators. When mapping these networks onto the brain with deep learning, differences in RSN topology were primarily observed in the DLPFC, parietal regions, and the ACC. In our previous work, significant differences were observed in both intra-network and inter-network connectivity in SAL[8]. Using independent component analysis of controls and PLWH, previous studies using RS-FC have shown the occipital lobe to be affected as well as reduced co-activation in occipital and parietal regions, possibly associated with VIS and PMN[19]. Chang et al.[20] also observed altered connectivity in numerous regions, including the DLPFC and parietal regions. Other studies have also shown altered connectivity in the ACC[21]. While these and our studies used different methodologies, the results consistently identified the SAL, VIS, and regions of the frontostriatal circuit as vulnerable to HIV independent of cognitive status.

The PMN, SAL, and FPN were the strongest predictors when comparing controls to PLWH CI with HIV status as the outcome. Similar to PLWH CN, topographic differences were primarily observed in the DLPFC, parietal regions, and the ACC. In addition, portions of the FPN including the RLPFC and parietal lobule were identified. Previously, Chaganti et al.[22] showed similar results when comparing controls to PLWH CI, with significant differences in both the SAL and executive networks. Similar to our current results, Chaganti et al.[22] also observed no significant differences in the somatosensory, DMN, and VAN networks when comparing these two groups.

With regards to cognitive impairment due to HIV (PLWH CN to PLWH CI), the strongest predictors were the REW, SAL, VAN, FPN, BGN, and VIS. Like the other comparisons, the

ACC and DLPFC were identified as regions with large differences in voxelwise analysis. In addition, this voxelwise analysis identified the caudate, globus pallidus, posterior putamen, ventromedial prefrontal cortex, amygdala, nucleus accumbens, and orbitofrontal regions. With regards to the basal ganglia, others have observed reductions in RS-FC in the caudate and globus pallidus[23].

The networks identified as the strongest predictors were important features for all three age groups. Our past research has demonstrated both HIV and age independently affect fMRI measures, but no interactions were observed[24]. Other studies have also observed that age and HIV were independent risk factors for developing HIV-associated neurocognitive disorders[25]. Voxelwise differences in RSNs generated with deep learning showed more variability with age than comparing weights at the network level. This is an indication that analysis of RSNs at the voxel level with deep learning could provide further insight into the effects of HIV on RSNs than analysis at the network ROI level. Other studies have also found age and task dependent variability in network activations[26]. The age variability in RSN topology and strength observed in our study is likely due to numerous factors, including cognitive reserve, legacy effects, response to cART, and/or compensation due to neuronal damage.

Several important networks, including SAL and FPN, are disproportionately affected by HIV. The SAL was a strong classifier across all age groups. The SAL network is believed to be responsible for the mediation of switching between the DMN and networks involved in executive function (FPN), and contributes to numerous complex brain functions[27]. In contrast, the controls and PLWH CI comparison and PLWH CN/PLWH CI comparison also showed the FPN as a strong predictor. The FPN is associated with numerous cognitive functions including attention, problem-solving, and working memory[28], each representing foundational components of complex, downstream cognitive operations. The FPN and SAL constitute two of the three RSNs that comprise the “triple network model”[28]. The triple network model consist of task negative states (DMN), task positive states (FPN), and switching states (SAL). Our results indicate that altered connectivity in both SAL and FPN underlies the shift from normative to impaired cognitive status among PLWH.

With regards to topographic changes, the ACC and DLPFC were important classifiers of HIV status and cognitive impairment status. The ACC and DLPFC are regions associated with the frontostriatal circuit, which is known to be associated with neurodegenerative and neuropsychiatric disorders[29]. In HIV, previous research has demonstrated altered connectivity in the DLPFC, dorsal caudate, and frontal and parietal regions connected to the DLPFC[30]. These changes have been observed in both cognitively normal and cognitively impaired PLWH. Studies have shown that the use of transcranial magnetic stimulation (TMS) leads to increased functional connectivity between the DLPFC and other regions of the frontostriatal circuit[31,32]. TMS directed at neural components of the FPN and/or SAL may help to mitigate the deleterious effects of HIV neuropathogenesis.

The main limitation of our study is the use of a cross-sectional research design. Research using prospective designs is needed to develop a clearer picture of the influence of HIV on RSNs. Further, cognitive impairment was assessed based on a summary measure of multiple

domains. Future studies should evaluate differences that are unique to specific domains. Future studies should also evaluate multiple feature selection algorithms to cross-check the predictive features identified in the current study. Lastly, studies are needed to understand the contribution of social determinants of health as salient features in studies of brain integrity among PLWH.

Conclusion

In this work, novel methods identified biomarkers of change in the functional organization of the brain in PLWH. We have identified RSNs that discriminate between controls, PLWH CN, and PLWH CI using machine learning for feature selection. Further, deep learning models identified anatomical regions where the largest changes in RSNs occurred. Finally, these analyses revealed patterns of change across age groups, suggesting that RSNs and cognitive changes for individuals may vary over time. This work provides group-level functional and anatomical inferences that could be foundations for future pharmacologic or rehabilitative interventions for PLWH. The deep learning models developed in this work can provide inferences for individuals, providing RSN maps that could be used in precision medical care.

Supplementary Material

Refer to Web version on PubMed Central for supplementary material.

Acknowledgements

The study was supported by grants from the National Institutes of Health (R01NR012657 and R01NR014449). The content is solely the responsibility of the authors and does not necessarily represent the official view of the NIH.

Conflicts of Interest and Source of Funding:

PHL, JSS, JJL, and/or Washington University in St. Louis may receive royalty income based on a technology developed by PHL, JSS, and JJL and licensed by Washington University to Sora Neuroscience. That technology is used in this research. This research was supported by the National Institutes of Health R01NR012657 and R01NR014449.

Data Availability

The datasets generated during and/or analyzed during the current study are not publicly available, but are available from the corresponding author on reasonable request.

References

1. HIV.gov. Global Statistics HIV.
2. Lentz MR, Kim WK, Lee V, et al. Changes in MRS neuronal markers and T cell phenotypes observed during early HIV infection. Neurology. 2009. doi:10.1212/WNL.0b013e3181a2e90a
3. Van Sighem A, Gras L, Reiss P, Brinkman K, De Wolf F. Life expectancy of recently diagnosed asymptomatic HIV-infected patients approaches that of uninfected individuals. AIDS. 2010. doi:10.1097/QAD.0b013e32833a3946
4. Heaton RK, Clifford DB, Franklin DR, et al. HIV-associated neurocognitive disorders persist in the era of potent antiretroviral therapy: Charter Study. Neurology. 2010;75(23):2087–2096. doi:10.1212/WNL.0b013e318200d727 [PubMed: 21135382]

5. Ferreira LK, Busatto GF. Resting-state functional connectivity in normal brain aging. Neurosci Biobehav Rev. 2013;37(3):384–400. [PubMed: 23333262]
6. Ortega M, Brier MR, Ances BM. Effects of HIV and combination antiretroviral therapy on cortico-striatal functional connectivity. AIDS. 2015. doi:10.1097/QAD.0000000000000611
7. Khosla M, Jamison K, Ngo GH, Kuceyeski A, Sabuncu MR. Machine learning in resting-state fMRI analysis. Magn Reson Imaging. 2019;64:101–121. [PubMed: 31173849]
8. Thomas JB, Brier MR, Snyder AZ, Vaida FF, Ances BM. Pathways to neurodegeneration: Effects of HIV and aging on resting-state functional connectivity. Neurology. 2013. doi:10.1212/WNL.0b013e318288792b
9. Urbanowicz RJ, Meeker M, La Cava W, Olson RS, Moore JH. Relief-based feature selection: Introduction and review. J Biomed Inform. 2018. doi:10.1016/j.jbi.2018.07.014
10. Passos IC, Mwangi B, Kapczinski F. Big data analytics and machine learning: 2015 and beyond. The Lancet Psychiatry. 2016;3(1):13–15. doi:10.1016/S2215-0366(15)00549-0 [PubMed: 26772057]
11. Luckett P, Paul RH, Navid J, et al. Deep Learning Analysis of Cerebral Blood Flow to Identify Cognitive Impairment and Frailty in Persons Living With HIV. J Acquir Immune Defic Syndr. 2019. doi:10.1097/QAI.0000000000002181
12. Paul RH, Cho KS, Luckett P, et al. Machine Learning Analysis Reveals Novel Neuroimaging and Clinical Signatures of Frailty in HIV. J Acquir Immune Defic Syndr. 2020. doi:10.1097/QAI.0000000000002360
13. Buckner RL, Roffman JL, Smoller JW. Brain Genomics Superstruct Project (GSP). Harvard Dataverse. doi:10.7910/DVN/25833
14. Morris JC. The Clinical Dementia Rating (CDR): Current version and scoring rules. Neurology. 2012;41(1):1588–1592. doi:10.1212/wnl.43.11.2412-a
15. Power JD, Mitra A, Laumann TO, Snyder AZ, Schlaggar BL, Petersen SE. Methods to detect, characterize, and remove motion artifact in resting state fMRI. Neuroimage. 2014. doi:10.1016/j.neuroimage.2013.08.048
16. Power JD, Cohen AL, Nelson SM, et al. Functional network organization of the human brain. Neuron. 2011;72(4):665–678. [PubMed: 22099467]
17. Seitzman BA, Snyder AZ, Leuthardt EC, Shimony JS. The State of Resting State Networks. Top Magn Reson Imaging. 2019. doi:10.1097/RMR.0000000000000214
18. Kira K, Rendell LA. A practical approach to feature selection. In: Proceedings of the Ninth International Workshop on Machine Learning. ; 1992:249–256. doi:10.1016/S0031-3203(01)00046-2
19. Wang X, Foryt P, Ochs R, et al. Abnormalities in Resting-State Functional Connectivity in Early Human Immunodeficiency Virus Infection. Brain Connect. 2011. doi:10.1089/brain.2011.0016
20. Chang L, Tomasi D, Yakupov R, et al. Adaptation of the attention network in human immunodeficiency virus brain injury. Ann Neurol. 2004. doi:10.1002/ana.20190
21. Jiang X, Barasky R, Olsen H, Riesenhuber M, Magnus M. Behavioral and neuroimaging evidence for impaired executive function in “cognitively normal” older HIV-infected adults. AIDS Care - Psychol Socio-Medical Asp AIDS/HIV. 2016. doi:10.1080/09540121.2015.1112347
22. Chaganti JR, Heinecke A, Gates TM, Moffat KJ, Brew BJ. Functional connectivity in virally suppressed patients with HIV-associated neurocognitive disorder: A resting-state analysis. Am J Neuroradiol. 2017. doi:10.3174/ajnr.A5246
23. Melrose RJ, Tinaz S, Castelo JMB, Courtney MG, Stern CE. Compromised fronto-striatal functioning in HIV: An fMRI investigation of semantic event sequencing. Behav Brain Res. 2008. doi:10.1016/j.bbr.2007.11.021
24. Ances BM, Vaida F, Yeh MJ, et al. HIV infection and aging independently affect brain function as measured by functional magnetic resonance imaging. J Infect Dis. 2010. doi:10.1086/649899
25. Van Gorp WG, Miller EN, Marcotte TD, et al. The relationship between age and cognitive impairment in HIV-1 infection: Findings from the multicenter AIDS cohort study and a clinical cohort. Neurology. 1994. doi:10.1212/wnl.44.5.929

26. Chang L, Holt JL, Yakupov R, Jiang CS, Ernst T. Lower cognitive reserve in the aging human immunodeficiency virus-infected brain. Neurobiol Aging. 2013. doi:10.1016/j.neurobiolaging.2012.10.012

27. Goulden N, Khusnulina A, Davis NJ, et al. The salience network is responsible for switching between the default mode network and the central executive network: Replication from DCM. Neuroimage. 2014. doi:10.1016/j.neuroimage.2014.05.052

28. Menon V Large-scale brain networks and psychopathology: A unifying triple network model. Trends Cogn Sci. 2011. doi:10.1016/j.tics.2011.08.003

29. Chudasama Y, Robbins TW. Functions of frontostriatal systems in cognition: Comparative neuropsychopharmacological studies in rats, monkeys and humans. Biol Psychol. 2006. doi:10.1016/j.biopsycho.2006.01.005

30. Du Plessis S, Vink M, Joska JA, Koutsilieri E, Stein DJ, Emsley R. HIV infection and the fronto-striatal system: A systematic review and meta-analysis of fMRI studies. AIDS. 2014. doi:10.1097/QAD.0000000000000151

31. Dunlop K, Woodside B, Lam E, et al. Increases in frontostriatal connectivity are associated with response to dorsomedial repetitive transcranial magnetic stimulation in refractory binge/purge behaviors. NeuroImage Clin. 2015. doi:10.1016/j.nicl.2015.06.008

32. Alkhasli I, Sakreida K, Mottaghy FM, Binkofski F. Modulation of fronto-striatal functional connectivity using transcranial magnetic stimulation. Front Hum Neurosci. 2019. doi:10.3389/fnhum.2019.00190

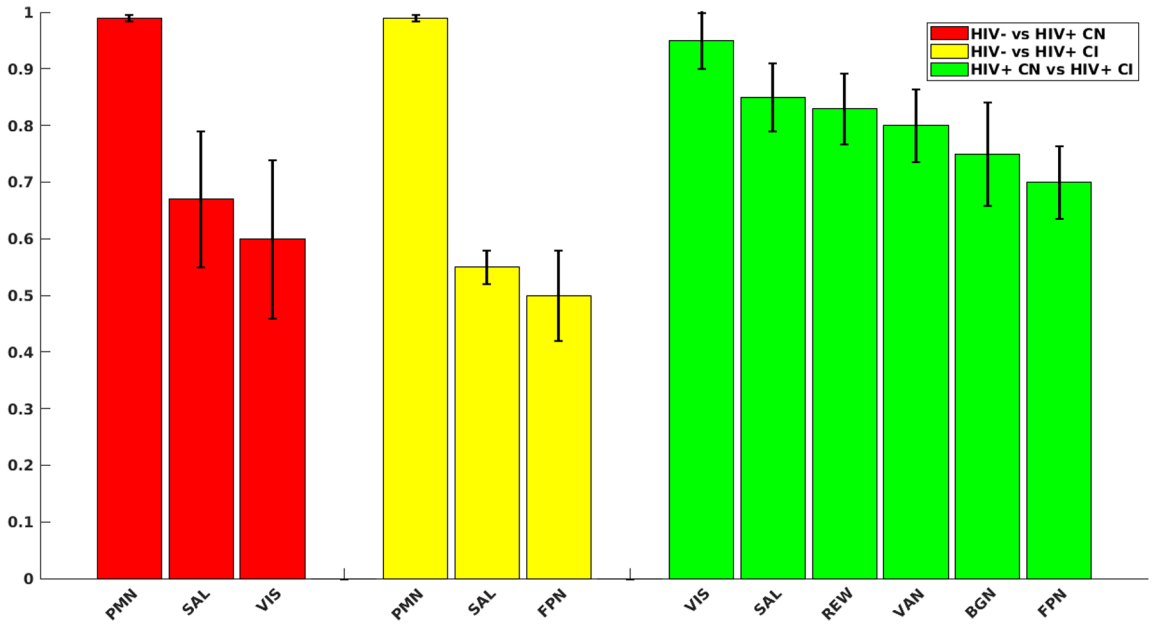

Figure 1: Strongest predictors for each group comparison.

Red bars are strongest predictors when comparing HIV status between controls and persons living with HIV (PLWH) cognitively normal. Yellow bars are strongest predictors when comparing HIV status between controls and PLWH cognitively impaired. Green bars are strongest predictors of cognitive impairment status between PLWH cognitively normal (CN) and PLWH cognitively impaired (CI). Black error bars indicate standard deviations of predictor strengths over 5 validation. Y-axis represents the predictive strength (weights) of the given networks. Weights were calculated by averaging the intra/inter network weights identified by the Relief algorithm and rescaled to a [0, 1] interval. Networks with weights close to one were the strongest predictors for a given outcome variable.

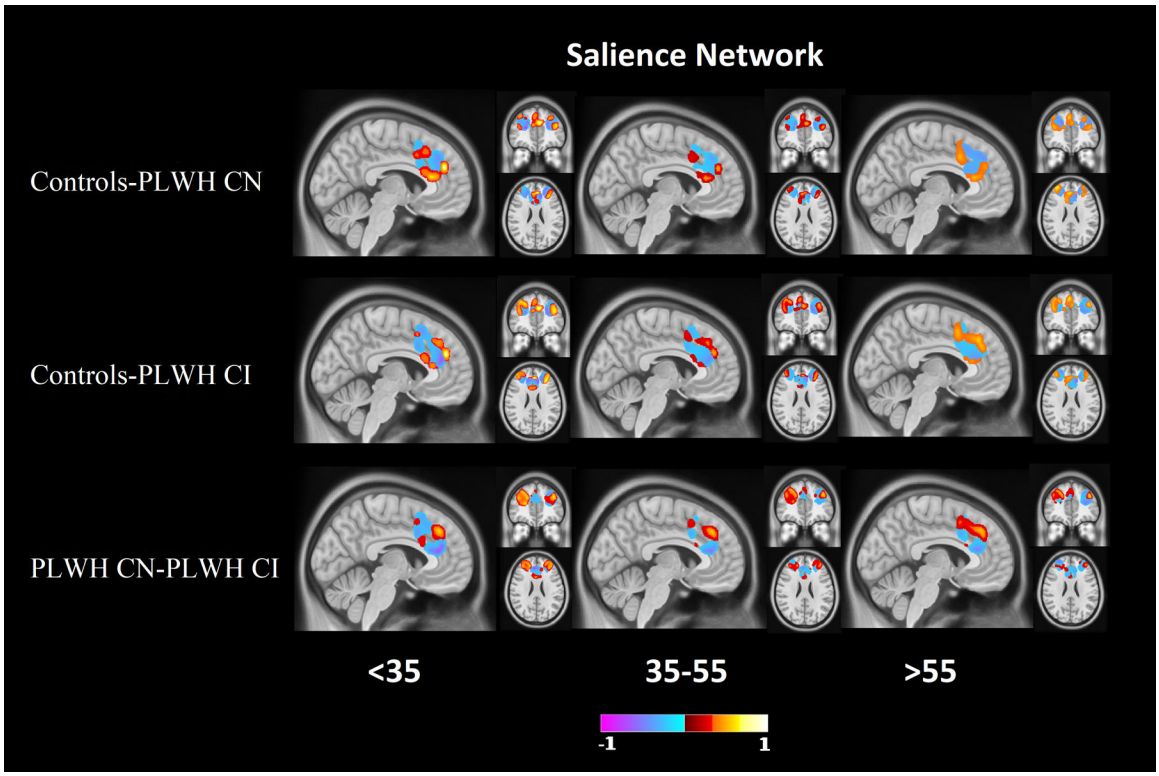

Figure 2: Difference maps for the salience (SAL) resting state network (RSN).

Difference maps for the SAL network at 0.2 minimum threshold, which was identified as a RSN with strong predictive ability to differentiate the three groups. Mixtures of higher and lower resting state functional connectivity (RS-FC) for group dependent regions were observed in the anterior cingulate cortex (ACC) and dorsolateral prefrontal cortex (DLPFC). Red indicates regions where controls have a stronger network signal compared to PLWH (top 2 rows), or PLWH CN have a higher network strength than PLWH CI (bottom row). Blue indicates regions where controls have a weaker network signal compared to PLWH (top 2 rows), or PLWH CN have a weaker network strength than PLWH CI (bottom row).

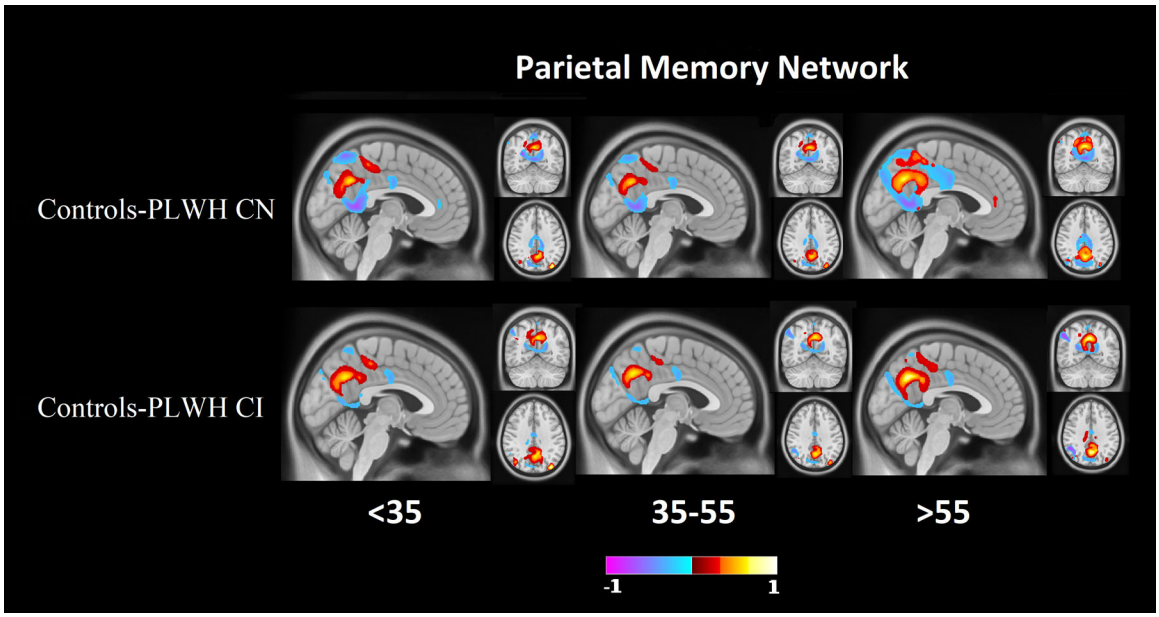

Figure 3: Difference maps for the parietal memory network (PMN).

Difference maps of PMN at 0.2 minimum threshold, identified as a strong predictor between controls and PLWH CN groups and controls and PLWH CI groups. Differences were primarily observed in parietal regions and the retrospenial cortex. Red indicates regions where controls have a stronger network signal compared to PLWH. Blue indicates regions where controls have a weaker network signal compared to PLWH.

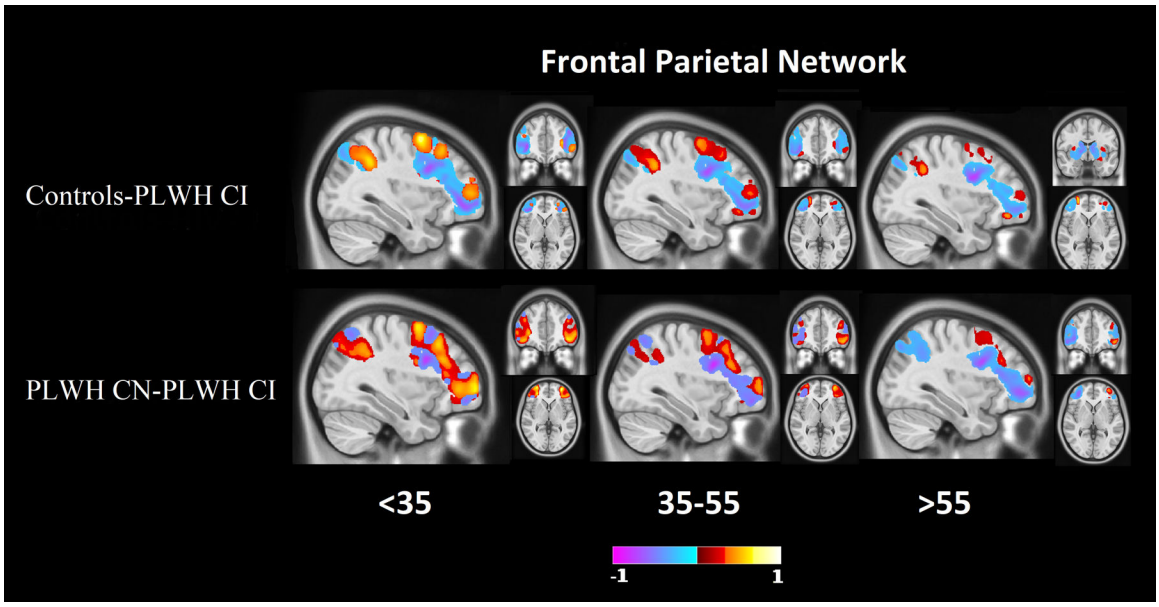

Figure 4: Difference maps for the frontal parietal network (FPN).

Difference maps of FPN at 0.2 minimum threshold, identified as a strong predictor between controls and PLWH CI groups and PLWH CN and PLWH CI groups. The DLPFC, rostral lateral prefrontal cortex, and portions of the parietal lobule showed large differences. Red indicates regions where controls have a stronger network signal compared to PLWH (top rows), or PLWH CN have a higher network strength than PLWH CI (bottom row). Blue indicates regions where controls have a weaker network signal compared to PLWH (top rows), or PLWH CN have a weaker network strength than PLWH CI (bottom row).

Table 1.

Demographics of cohort

	Controls, N=1509	PLWH CN, N=181	PLWH CI, N=116	p value
Age (years) , mean (SD)	45.4 ± 23.6	50.5 ± 12.9	44.6 ± 14.4	0.17
Sex (% Male)	62%	65%	69%	0.20
Education, mean (SD) (years)	14.1 ± 2.4	13.9 ± 2.4	13.7 ± 2.3	0.18
Race (% Caucasian)	79%	40%	27%	<0.001
Race (% African American)	10%	59%	73%	<0.001
Race (% Other)	11%	1%	0%	<0.001
Duration of Infection (years), mean (SD)		15.1 ± 8.2	15.1 ± 7.3	0.97
Current CD4 cells/μl, median (IQR)		595 (415)	614 (390)	0.31

SD=standard deviation, cART=combination antiretroviral therapy, IQR=interquartile range.